tvst

New Developments in Vision Research

Choroidal Vessel and Stromal Volumetric Analysis After Photodynamic Therapy or Focal Laser for Central Serous Chorioretinopathy

Chikako Hara[1,2], Kazuichi Maruyama[1,3,4], Taku Wakabayashi[1], Shiyi Liu[5], Zaixing Mao[5], Ryo Kawasaki[1,6], Zhenguo Wang[5], Kinpui Chan[5], and Kohji Nishida[1,4]

[1] Department of Ophthalmology, Graduate School of Medicine, Osaka University, Suita, Osaka, Japan
[2] Department of Advanced Device Medicine, Graduate School of Medicine, Osaka University, Suita, Osaka, Japan
[3] Department of Vision Informatics, Graduate School of Medicine, Osaka University, Suita, Osaka, Japan
[4] Integrated Frontier Research for Medical Science Division, Institute for Open and Transdisciplinary Research Initiatives (OTRI), Osaka University, Suita, Osaka, Japan
[5] Topcon Advanced Biomedical Imaging Laboratory, Oakland, NJ, USA
[6] Department of Innovative Visual Science, Graduate School of Medicine, Osaka University, Suita, Osaka, Japan

Correspondence: Chikako Hara, Department of Ophthalmology, Graduate School of Medicine, Osaka University, Room E7, 2-2 Yamadaoka, Suita, Osaka 565-0871, Japan. e-mail: chikako.ueno@ophthal.med.osaka-u.ac.jp

Received: June 12, 2023
Accepted: September 22, 2023
Published: November 20, 2023

Keywords: choroidal volume; central serous chorioretinopathy; photodynamic therapy; deep learning; laser photocoagulation

Citation: Hara C, Maruyama K, Wakabayashi T, Liu S, Mao Z, Kawasaki R, Wang Z, Chan K, Nishida K. Choroidal vessel and stromal volumetric analysis after photodynamic therapy or focal laser for central serous chorioretinopathy. Transl Vis Sci Technol. 2023;12(11):26, https://doi.org/10.1167/tvst.12.11.26

Purpose: To utilize volumetric analysis to quantify volumetric changes in choroidal vessels and stroma after photodynamic therapy (PDT) and focal laser photocoagulation (PC) for central serous chorioretinopathy (CSCR).

Methods: This retrospective, comparative study included 58 eyes (58 patients) with CSCR (PC, 33 eyes; PDT, 25 eyes) followed up with swept-source optical coherence tomography at 3 months after treatment. Three-dimensional (3D) choroidal vessel and stromal volumes in each area of the central 1.5-mm-diameter circle, the torus-shaped area with 6-mm-diameter circle excluding the area of the central 1.5-mm-diameter circle, and the treated area of the Early Treatment Diabetic Retinopathy Study (ETDRS) grid centered at the fovea were analyzed using a deep learning–based method. Changes in volume at baseline and 1 and 3 months after treatment were compared.

Results: The mean patient age was 49.3 $\pm$ 10.5 years. In the central 1.5-mm-diameter circle, the mean vessel and stromal volume rates significantly decreased after the treatment in both the PDT and PC groups ($P = 0.00029$ and $P = 0.0014$, respectively), and significant differences between the PDT and PC groups of continuous variables within times were observed in both volumes ($P = 0.024$ and $P = 0.037$, respectively). In the torus-shaped area and treated area, the PDT and PC groups both showed similar decreases in vessel and stromal volume over time.

Conclusions: In the 3D optical coherence tomography volumetric analysis, both PDT and focal PC reduced choroid vessel volume in eyes with CSCR.

Translational Relevance: This new finding is useful in elucidating the pathogenesis and healing mechanisms of CSCR.

Introduction

Central serous chorioretinopathy (CSCR) is a chorioretinal disorder that causes serous retinal detachment.[1] Although its pathogenesis is not fully understood, it involves a thickened choroid, hyperpermeability of choroidal vessels, large choroidal vessel dilatation in the middle and Haller's layer, and consequent decompensation of the retinal pigment epithelium (RPE).[2–6] Treatments for CSCR include laser photocoagulation (PC)[7,8] and photodynamic therapy (PDT). PC is applied at the leak spot away from the fovea,[8,9] whereas PDT is indicated in cases with foveal leakage.[10–13] Previous studies have reported that the central choroidal thickness significantly reduced

after PDT[10–14] but not after PC.[6] However, most of these studies analyzed choroidal thickness under the fovea on one cross-sectional B-scan on optical coherence tomography (OCT). As the choroid is a three-dimensional (3D) tissue containing various diameters of blood vessels and stroma, cross-sectional OCT alone does not represent the entire pathology of CSCR. In addition, hyperpermeable choroidal vessels and leakage spots are present not only in the subfoveal region but also in various extrafoveal regions. Therefore, analysis of the subcentral choroid alone may be insufficient to analyze the pathogenesis of CSCR.

Various methods of 3D analysis have revealed clinically relevant structural details, including choroidal volumes, that two-dimensional (2D) analysis could not reveal. Recently, we reported the quantitative 3D volume analysis of healthy and diseased choroids using an artificial intelligence (AI) processing method.[15] This method can be applied to pre-obtained OCT images, thereby offering widespread applicability, and OCT images can be utilized for quantitative analysis of the choroidal structure, including vessel and stromal volume. Thus, this method might elucidate the pathogenesis of CSCR and the treatment responsiveness of the choroid after treatment.

Here we investigated the quantitative changes of choroidal structure in eyes with CSCR before and after laser photocoagulation and PDT using this new method.

Methods

This retrospective study was conducted at the Osaka University Hospital. The study was approved by the Institutional Review Board of the Osaka University Graduate School of Medicine (Project #09260-5, 17279-3) and followed the tenets of the Declaration of Helsinki. This is a retrospective case series study; thus, the requirement for informed consent was waived.

This study included 58 eyes of 58 patients with CSCR who were treated by PC or PDT at the leak points associated with CSCR and were evaluated with DRI OCT swept-source optical coherence tomography (SS-OCT) (Topcon, Tokyo, Japan) at the 3-month follow-up. All patients underwent SS-OCT, which acquires 12 × 9-mm OCT volumes (512 A-lines per B-scan and 256 B-scans per volume) over the macular area to provide 3D volumetric information at pretreatment and at 1 month and 3 months after treatment. The following patients were excluded: (1) cases in which the presence of choroidal neovascularization could not be ruled out on multimodal imaging; (2) cases with other retinal diseases, including diabetic retinopathy, retinal venous occlusion, and ocular inflammation; (3) cases with high myopia (> −6 diopters); and (4) those who had SS-OCT images of the choroid that were indistinct due to large pigment epithelium detachment and subretinal fibrin. The patients who had previously been treated with PC or PDT and developed subretinal fluid recurrence were included. Ophthalmic examinations, including best-corrected visual acuity (BCVA) using the Landolt C chart, fundus examination, color fundus photography, and SS-OCT, were performed for all patients at all visits. Fluorescein and indocyanine green angiography was performed in all patients before treatment. Central retinal thickness (CRT) was defined as the distance between the internal limiting membrane and the presumed RPE at the fovea and was assessed using SS-OCT. Central choroidal thickness (CCT) was defined as the distance between the presumed RPE and chorioscleral interface at the fovea and was evaluated using SS-OCT.

Diagnosis and Treatment

Diagnosis of CSCR was based on multimodal imaging analysis, including leakage on fluorescein angiography (FA), permeability of choroidal vessels on indocyanine green angiography (ICGA), and serous retinal detachment (subretinal fluid) on OCT.[16] Decisions regarding treatment approaches were made in accordance with standard therapeutic practice.[17] When FA showed pinpoint leak spots away from the fovea, the eyes were treated with conventional focal PC (PC group). If the leak point on FA was diffuse or near (<200 μm) or at the fovea, the eyes were treated with PDT (PDT group). Conventional focal PC in the PC group was performed using a yellow laser (561 μm; ZEISS Group, Dublin, CA) with a spot size of 50 to 100 μm at a power of 80 to 100 mW, with an application time of 0.15 seconds. The endpoint of the PC was a grayish color change in the RPE. PDT was performed using 6 mg/m^2 verteporfin (Visudyne; Novartis, Basel, Switzerland). The verteporfin was infused over a period of 10 minutes, and a ZEISS 689-nm laser system was used at an irradiance of 600 mW/cm^2 over a 70-second exposure time, which is shorter than the normal exposure time (83 seconds), starting 15 minutes after the start of the infusion. The PDT spot size was the largest circle determined by the region of the leakage area on the FA image or the area of hyperpermeability on indocyanine angiography, or both, which did not include an additional margin. The actual irradiated

circle was recorded on the FA image; thus the Early Treatment Diabetic Retinopathy Study (ETDRS) grid centered at the fovea was superimposed on it to determine the treated area.

Quantitative Visualization of the Choroidal Structure

Details regarding the image enhancement and vessel segmentation processes have been provided in a previous report.[15] The SS-OCT images of 12 × 9-mm B-scans over the macular area were used to generate the 3D vascular structure within the choroid for quantitative analysis. First, to enhance the image quality and aid accurate choroidal vessel segmentation, the original volumetric OCT scans were subjected to a series of preprocessing methods. Noise reduction was first implemented by a custom deep learning–based noise reduction algorithm,[18–20] which used a U-Net model trained on noisy images from the Topcon DRI OCT Triton. Shadow reduction was then applied on each A-line to neutralize the dark appearance of shadow artifacts in the deep layers. In order to improve the vessel visualization, especially in the deep choroid, attenuation compensation and contrast enhancement with a local Laplacian filter[21,22] were applied at the end of preprocessing.

The preprocessed OCT scans were then segmented using the Topcon Advanced Boundary Segmentation (TABS) algorithm[23] (version 10.16.003.02) with manual correction for errors if required, and choroidal vessels were segmented using a fully automated approach via a composite method that utilizes the contrast difference between the choroidal vessels and stroma.[24–27] A fully automated composite segmentation method was utilized that fused both local and global thresholding techniques. In terms of local thresholding, B-scans and C-scans provide distinct perspectives that are crucial for effective segmentation of choroidal vessels. B-scan segmentation,[24,28] recognized for its simplicity, is routinely employed, whereas C-scan segmentation[26] enhances vessel connectivity, given that shadows from retinal vessels have been mitigated during preprocessing. Moreover, global thresholding techniques[29] surpass local ones when it comes to segmenting large, dilated vessels in pathological conditions. Our combined approach facilitates more precise and resilient choroidal vessel segmentation. The composite segmentation results yield a detailed 3D depiction of the choroidal vessel architecture. Volume measurements are ascertained by multiplying pixel resolution with the number of pixels.

Segmented information about the choroidal vessels was then fed directly into imaging software (VisIt),[30]

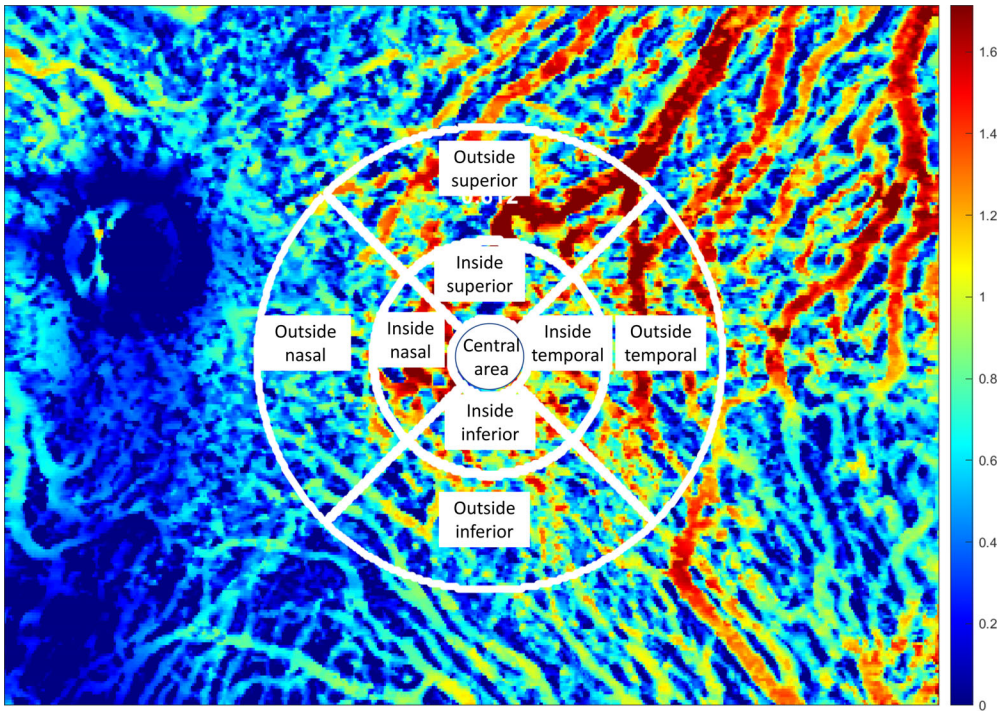

Figure 1. Overlay of an ETDRS grid on a 3D segmentation map.

the 3D vascular structure of the choroid was visualized, and a 3D segmentation map was created. This 3D segmentation map also provides quantification of the total choroid and choroidal vessels, and the choroidal stromal volume can be calculated by subtracting the vascular volume from the total choroidal volume. The overlay of an ETDRS grid centered at the fovea on a 3D segmentation map can be applied to derive regional quantifications and reveal focal changes in vessel and stromal pathology (Fig. 1).

Analysis of Acquired Data

The vessel and stromal volumes were measured in the central 6-mm-diameter circle of the ETDRS chart. Each volume was calculated for the entire circle and each of the nine individual areas (Fig. 1). We evaluated the volume of the 1.5-mm-diameter central circle, the torus-shaped area (the area with 6-mm-diameter circle excluding the area of the central 1.5-mm-diameter circle), and the treated area. The treated areas were determined to be those where photocoagulation was performed or PDT was irradiated. The most widely irradiated area was selected when it covered two or more areas. The change in volume was evaluated as the ratio from pretreatment.

Statistical Analysis

BCVA was converted to logarithm of the minimum angle of resolution (logMAR) units for statistical analysis. A generalized liner mixed-effects model was used to assess the differences between PDT and PC and changes over time (pretreatment and 1 month and 3 months posttreatment). The model was fitted with treatment (PDT and PC) and time as fixed effects and time and an individual as the random effects. For all analyses, $P < 0.05$ was considered statistically significant when adjusting for multiple comparisons.

Results

Overall, 58 eyes of 58 patients were included in this study; 42 patients were male (72%), and 16 patients were female (28%). The mean age was 73.9 ± 8.8 years. Six patients (10.3%) received systemic administration of steroids. Further, 33 eyes (57%) were treated with conventional PC (PC group), and the remaining 25 eyes (43%) were treated with PDT (PDT group). For the duration of CSCR, based on self-reports and existing data, 19 eyes in the PC group were diagnosed within 6 months (minimum 1 month), three eyes within 6 months to 1 year, and nine eyes over 1 year later. In the PDT group, three eyes were diagnosed within 6 months (minimum 2 months), nine eyes within 6 months to 1 year, and 10 eyes over 1 year later.

Baseline characteristics of each group are presented in Table 1. Significant differences were observed in sex, but no significant differences were noted between the two groups in other variables, including age, systemic steroid administration, BCVA, mean CRT, or CCT. As it has been reported that no sex-related difference exists in choroidal thickness, we do not believe the

Table 1. Patient Characteristics at Pretreatment

	Total	PC	PDT	*P* (PC Group vs. PDT Group)
Eyes/patients, *n*	58/58	33/33	25/25	
Age (y), mean ± SD	49.2 ± 10.5	46.9 ± 7.8	52.3 ± 12.8	0.0516
Male eyes, *n* (%)	42 (72.4)	28 (84.9)	14 (56.0)	0.0197*
Systemic steroid administration, *n* (%)	6 (10.3)	3 (9.1)	3 (12)	1.00
BCVA (logMAR), mean ± SD	0.09 ± 0.20	0.07 ± 0.14	0.12 ± 0.25	0.36
CRT (µm), mean ± SD	419.7 ± 176.4	444.2 ± 188.3	387.2 ± 157.2	0.23
CCT (µm), mean ± SD	393.2 ± 97.9	407.7 ± 97.3	374.0 ± 97.1	0.196
Vessel volume (mm^3), mean ± SD				
Central	0.14 ± 0.05	0.14 ± 0.05	0.13 ± 0.043	0.497
Torus-shaped area	14.16 ± 4.01	14.16 ± 3.53	12.64 ± 4.50	0.155
Treated area	0.55 ± 0.39	0.70 ± 0.34	0.35 ± 0.36	0.0004*
Stroma volume (mm^3), mean ± SD				
Central	0.14 ± 0.04	0.15 ± 0.04	0.13 ± 0.04	0.093
Torus-shaped area	13.35 ± 4.15	13.66 ± 2.85	12.62 ± 4.46	0.280
Treated area	0.53 ± 0.36	0.67 ± 0.31	0.34 ± 0.34	0.0003*

*$P < 0.05$.

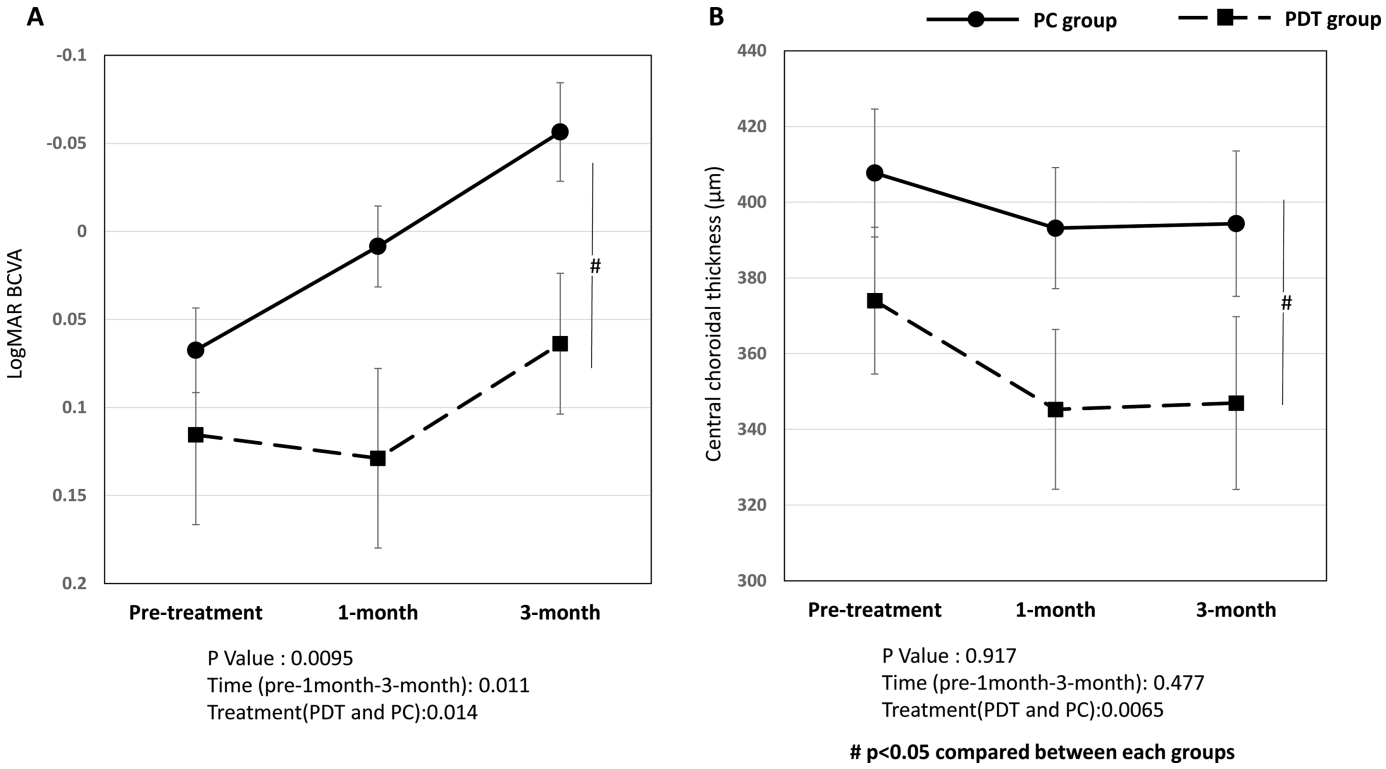

Figure 2. Time course of mean BCVA (**A**) and CCT (**B**) in all eyes after laser PC or PDT.

baseline difference had any effect.[31] For the vessel and stromal volumes at baseline of the central 1.5-mm-diameter circle and the torus-shaped area no significant difference was observed between the PDT and PC groups. However, these volumes at the treated area in the PC group were significantly greater than those in the PDT group because the measurement area was originally larger in the peripheral area than in the center circle. Moreover, more eyes were treated near the center circle in the PDT group, and more eyes were treated near the peripheral area in the PC group (Table 1).

Changes in the mean BCVA and CCT are shown in Figure 2. The logMAR BCVA improved from 0.07 ± 0.14 at baseline to 0.009 ± 0.13 at 1 month and –0.06 ± 0.16 at 3 months in the PC group. In the PDT group, the logMAR BCVA values were 0.12 ± 0.25, 0.13 ± 0.25, and 0.06 ± 0.20 at baseline and at 1 month and 3 months after treatment, respectively. The logMAR BCVA was significantly better in the PC group than in the PDT group ($P = 0.014$) (Fig. 2A).

CCT decreased from 408 ± 97 μm at baseline to 393 ± 92 μm and 394 ± 110 μm at 1 month and 3 months after treatment, respectively, in the PC group and decreased from 374 ± 97 μm to 345 ± 106 μm and 347 ± 114 μm at 1 month and 3 months after the treatment, respectively, in the PDT group. Significant decreases were noted in the PDT group compared to the PC group ($P = 0.0065$) (Fig. 2B).

Changes in Vessel and Stromal Volume of the Choroid

The time course of changes in vessel and stromal volumes are shown in Figure 3 and Table 2. In the central 1.5-mm-diameter circle of the ETDRS chart, the mean vessel and stromal volume rate significantly decreased after treatment in both PDT and PC groups ($P < 0.0001$ and $P < 0.0002$ for vessel and stroma, respectively). Significant differences between the PDT and PC groups of continuous variables were observed in both vessel and stromal volume ($P = 0.024$ and $P = 0.037$, respectively) (Figs. 3A, 3B). In the torus-shaped area, the PDT and PC groups both showed a similar decrease in vessel and stromal volume over time (time: $P < 0.0001$ and $P < 0.0001$, respectively; treatment: $P = 0.177$ and $P = 0.209$, respectively) (Figs. 3C, 3D). In the treated area of the ETDRS chart, no difference between the PDT and PC groups was observed, similar to the torus-shaped area; both vessel and stromal volumes decreased over time. (time: $P < 0.0001$ and $P < 0.0001$, respectively; treatment: $P = 0.166$ and $P = 0.233$, respectively) (Figs. 3E, 3F, 4, 5).

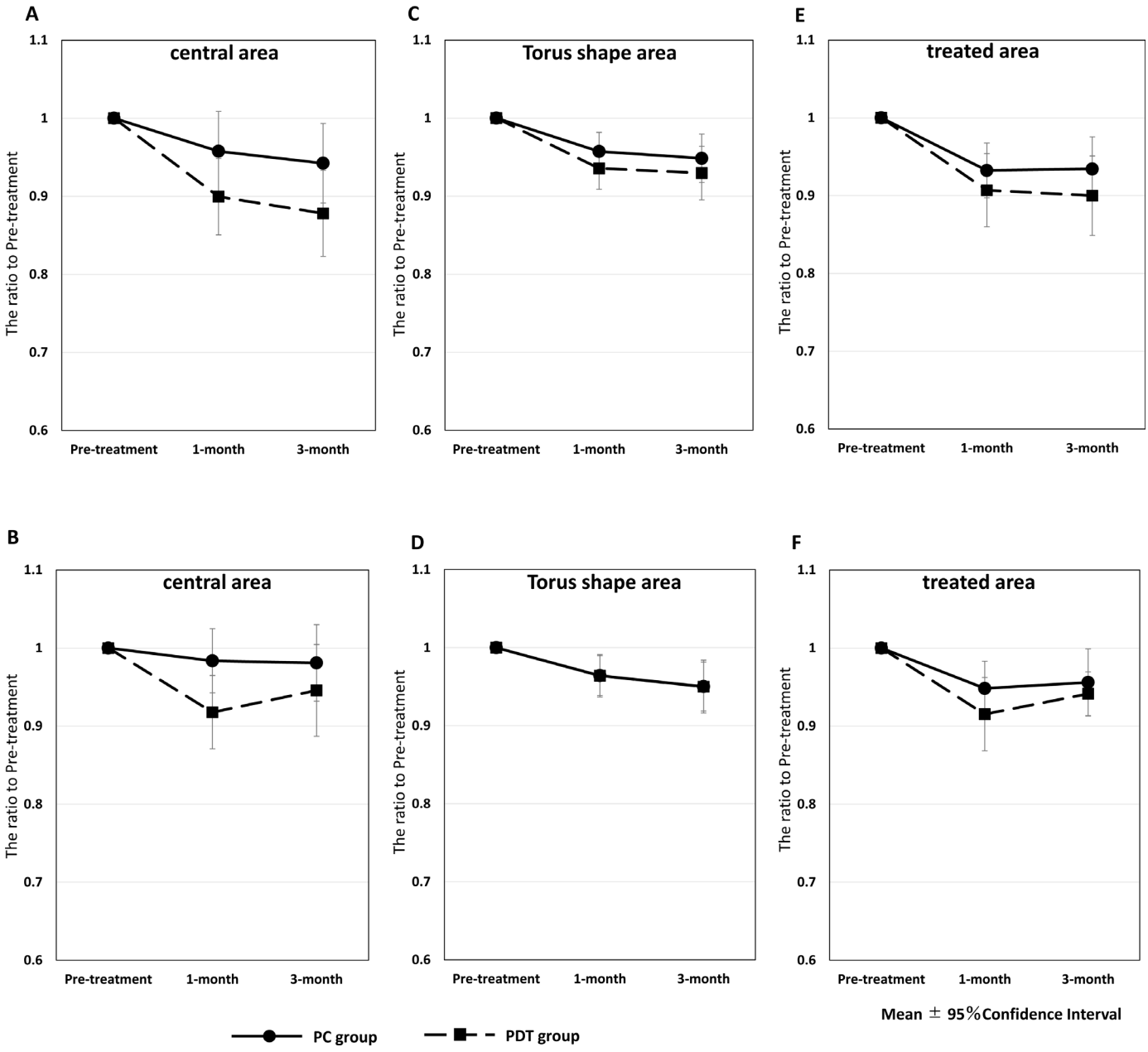

Figure 3. Time course of the mean ratio of vessel volume (**A**, **C**, **E**) and stromal volume (**B**, **D**, **F**) to pretreatment in the central circle, torus-shaped area, and treated area in all eyes after laser PC or PDT.

Discussion

To the best of our knowledge, at the time of this writing, this is the first report of 3D analysis to evaluate choroidal vascular and stromal volumes separately in the eyes of patients with CSCR who received PC or PDT. The noteworthy findings obtained with our 3D analysis revealed that choroidal vessel volume in eyes with CSCR decreases after not only PDT but also PC. These new findings were obtained using our novel methods of analyzing choroidal vessels and stroma separately and using 3D information in areas of particular interest.[15] Vessel volume maps that can be formatted to scrutinize small, selected quadrants allowed us to detect focal pinpoint changes in the choroidal vasculature.

Many previous studies have reported choroidal changes in CSCR using cross-sectional (2D) OCT images. According to these studies, CCT decreases to 80% to 90% compared with baseline following PDT,[6,12,14,32] whereas CCT does not decrease after PC.

Table 2. Changes in Vessel and Stroma Volume After Treatment

	Ratio to Pretreatment						
	PDT		PC				
	1 Month	3 Months	1 Month	3 Months	*P*	*P* (Time: Pretreatment, 1 Month, 3 Months)	*P* (Treatment: PDT vs. PC)
1.5-mm-Diameter Central Circle							
Vessel	0.90	0.88	0.96	0.94	0.192	<0.0001*	0.024*
Stroma	0.92	0.95	0.98	0.98	0.307	0.0002*	0.037*
Torus-Shaped Area (1.5–6 mm)							
Vessel	0.94	0.93	0.96	0.95	0.528	<0.0001*	0.178
Stroma	0.93	0.95	0.96	0.95	0.928	<0.0001*	0.303
Treated Area							
Vessel	0.90	0.90	0.93	0.93	0.356	<0.0001*	0.166
Stroma	0.92	0.94	0.95	0.96	0.580	<0.0001*	0.233

*$P < 0.05$.

In accordance with these reports, our study showed that the CCT was significantly reduced to 92% in the PDT group, although there was no significant reduction in CCT in the PC group. However, notably, with the 3D analysis of our study, both vessel and stromal volume significantly decreased in the PC group, although no significant difference in CCT was observed in the 2D images. CCT is usually measured at only one point, the fovea. In this study, the rate of decrease in vessel volume in the PC group was significantly lower than that in the PDT group. Therefore, CCT measurement alone may not be useful for detecting potential changes in the choroid in the PC treatment group. In the torus-shaped area and treated area of the PC group, both vessel and stromal volumes significantly decreased, similar to the degree observed in the PDT group. More eyes underwent treatment[35] in the central region in the PDT group. This may account for the lower rate of reduction in vessel volume in the central region in the PC group than in the PDT group, and PC is also thought to decrease vessel volumes similar to PDT. This may be related to the fact that the largest choroidal volume anatomically was observed at the fovea, and, therefore, the vessel and stromal volume are larger. The mechanism of the SRF resolution after PC treatment remains unclear, although it has been postulated that PC may close the rip of the RPE and stimulate the pump function of the RPE near the rip.[7,33,34] Our findings may add some insights into the PC-induced resolution of CSCR. The mechanism of PDT in CSCR is presumably based on the formation of free radicals on the irradiated area, which leads to vascular endothelium remodeling and decreased choroidal vessel dilation. Previously, the mechanism of PC had been thought to only close the rip of the RPE; however, PC may also have the effect of vascular remodeling and the reduction of choroidal hyperpermeability or congestion associated with CSCR. It was thought that PDT is more effective in improving the pathogenesis of CSCR because it reduces choroidal thickness, but a similar effect can be expected with PC. Therefore, if the leakage point is far from the central fovea, PC may be a good option.

In a recent study that analyzed choroidal volume change using the 3D method, carried out using the choroid quantification program provided by ZEISS after PDT for CSCR,[35] the choroidal volume in the irradiated area significantly decreased, but not in non-irradiated peripheral areas with PDT. In the PDT group in the present study, vessel volume significantly decreased in all areas, but the vessel volume decreased at a higher rate in the treated area than in the torus-shaped area. This result suggests that the decrease was more pronounced in the treated area and less pronounced outside the treated area. Some previous studies quantitatively analyzed the vessel and stroma of the choroid separately, as in the present study,[24,36–38] and examined their changes after PDT treatment.[39,40] However, these studies reported choroidal vascularity in 2D without the visualization of vasculature,[25] or they obtained only 3D visualizations in normal subjects.[29,41–44] Although two studies[26,29] reported a significant decrease in the luminal area, the stromal area did not decrease in their studies. In our study, the stromal volume significantly decreased in the central and treated areas, potentially due to our novel and accurate measurement of vessel and stromal volumes using 3D analysis. These results suggest the advantage of measuring choroidal vessel and stromal volumes separately when evaluating the response to treatment in patients with CSCR.

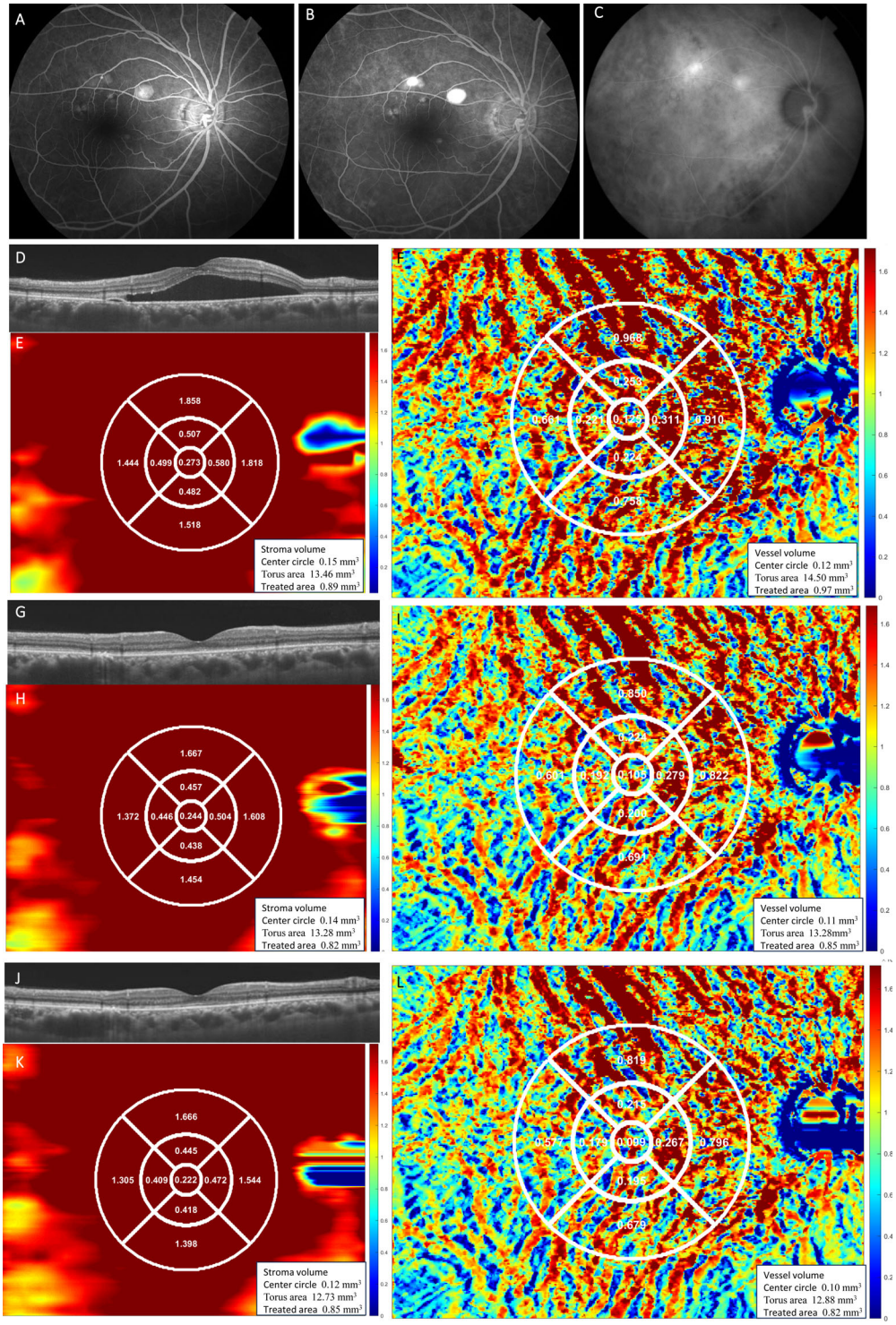

Figure 4. A 49-year-old man was treated with laser PC for CSCR. Fluorescein angiography (A, early phase; B, late phase) showed leakage superior to the macula, and indocyanine green angiography showed hyperpermeability (C). Subretinal fluid was observed at baseline (D) and resolved at 1 month (G) and 3 months (J) after laser PC at the leakage spot. Color maps show choroidal volume (E, H, K) and vessel volume (F, I, L) at baseline and at 1 month and 3 months after treatment. Clear decreases in choroidal and vessel volumes were observed around the irradiated area (outside superior) at 1 month and 3 months after treatment. The vessel and stroma volume in the central circle at 3 months after treatment deceased to 0.80 and 0.80, respectively, compared to pretreatment. In the treated area (outside superior), the vessel and stroma volumes at 3 months decreased to 0.85 and 0.95, respectively, compared to pretreatment.

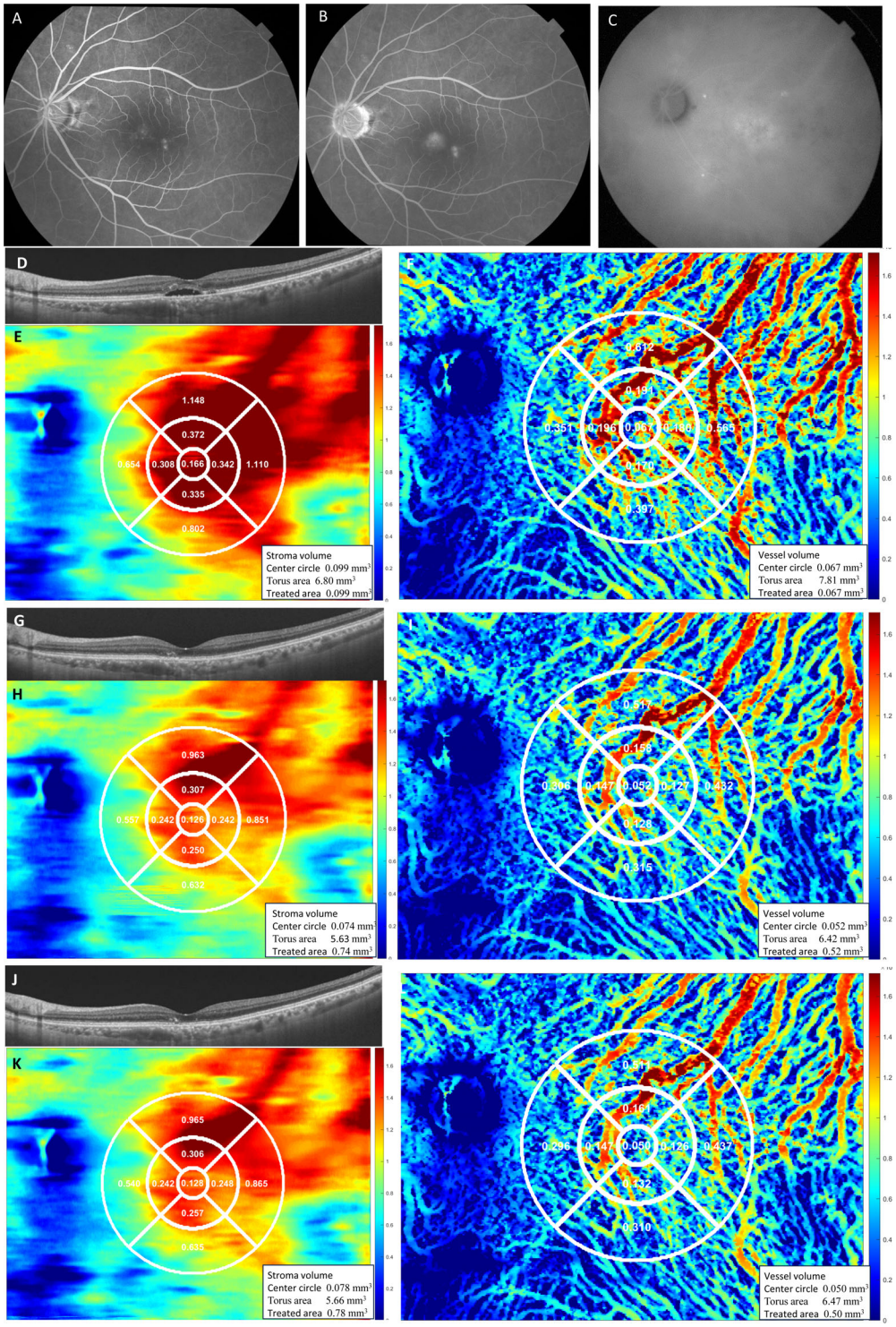

Figure 5. A 70-year-old man was treated with PDT for chronic CSCR. Fluorescein angiography (A, early phase; B, late phase) shows leakage near the macula, and indocyanine green angiography shows hyperpermeability near the macula (C). Subretinal fluid was observed at pretreatment (D) and resolved at 1 month (G) and 3 months (J) after photodynamic therapy for a circle with a diameter of 1000 µm in the central 1.5-mm-diameter circle. Color maps show choroidal volume (E, H, K) and vessel volume (F, I, L) at baseline and at 1 month and 3 months after treatment. A clear decrease in choroidal and vessel volumes was observed around the irradiated area at 3 months after treatment.

The limitations of this study include its retrospective design, relatively small sample size, and a short observation period after treatment. In addition, our current methods require manual inspection to obtain layer segmentation in some cases. In this study, manual correction for layer segmentation was required in only two cases (3.4%), so we believe that the impact of manual correction bias on CSC analysis was not significant. However, our research to overcome the current methodological limitations is ongoing, and further development toward fully automated segmentation is expected in the near future. Most importantly, the ability to observe detailed choroidal changes with this method increases the likelihood of elucidating the pathophysiology and clarifying whether or not PC and PDT, which have been used in the treatment of CSCR, are helping to improve the pathophysiology. Additionally, this new method of detailed choroidal analysis can elucidate the pathogenesis of CSCR, as well as other choroidal diseases.

In conclusion, our study determined that the choroidal vessel volume in patients with CSCR decreased in response to PDT and PC, especially in the treated area, due to our 3D analysis of the choroid. These results may provide new insights into the response to CSCR treatment.

Acknowledgments

Supported by a Grant-in-Aid for Scientific Research (20K09772) from the Ministry of Education, Science and Culture of Japan.

Disclosure: **C. Hara**, None; **K. Maruyama**, None; **T. Wakabayashi**, None; **S. Liu**, None; **Z. Mao**, None; **R. Kawasaki**, None; **Z. Wang**, None; **K. Chan**, None; **K. Nishida**, None

References

1. Gass JD. Pathogenesis of disciform detachment of the neuroepithelium. *Am J Ophthalmol*. 1967;63(suppl. 3):S1–S139.
2. Prünte C, Flammer J. Choroidal capillary and venous congestion in central serous chorioretinopathy. *Am J Ophthalmol*. 1996;121(1):26–34.
3. Imamura Y, Fujiwara T, Margolis R, Spaide RF. Enhanced depth imaging optical coherence tomography of the choroid in central serous chorioretinopathy. *Retina*. 2009;29(10):1469–1473.
4. Baek J, Lee JH, Jung BJ, Kook L, Lee WK. Morphologic features of large choroidal vessel layer: age-related macular degeneration, polypoidal choroidal vasculopathy, and central serous chorioretinopathy. *Graefes Arch Clin Exp Ophthalmol*. 2018;256(12):2309–2317.
5. Maruko I, Iida T, Sugano Y, Ojima A, Sekiryu T. Subfoveal choroidal thickness in fellow eyes of patients with central serous chorioretinopathy. *Retina*. 2011;31(8):1603–1608.
6. Maruko I, Iida T, Sugano Y, Ojima A, Ogasawara M, Spaide RF. Subfoveal choroidal thickness after treatment of central serous chorioretinopathy. *Ophthalmology*. 2010;117(9):1792–1799.
7. Leaver P, Williams C. Argon laser photocoagulation in the treatment of central serous retinopathy. *Br J Ophthalmol*. 1979;63(10):674–677.
8. Ficker L, Vafidis G, While A, Leaver P. Long-term follow-up of a prospective trial of argon laser photocoagulation in the treatment of central serous retinopathy. *Br J Ophthalmol*. 1988;72(11):829–834.
9. Yap EY, Robertson DM. The long-term outcome of central serous chorioretinopathy. *Arch Ophthalmol*. 1996;114(6):689–692.
10. Chan WM, Lam DS, Lai TY, Tam BS, Liu DT, Chan CK. Choroidal vascular remodelling in central serous chorioretinopathy after indocyanine green guided photodynamic therapy with verteporfin: a novel treatment at the primary disease level. *Br J Ophthalmol*. 2003;87(12):1453–1458.
11. Taban M, Boyer DS, Thomas EL, Taban M. Chronic central serous chorioretinopathy: photodynamic therapy. *Am J Ophthalmol*. 2004;137(6):1073–1080.
12. Fujita K, Imamura Y, Shinoda K, et al. One-year outcomes with half-dose verteporfin photodynamic therapy for chronic central serous chorioretinopathy. *Ophthalmology*. 2015;122(3):555–561.
13. Park W, Kim M, Kim RY, Park YH. Comparing effects of photodynamic therapy in central serous chorioretinopathy: full-dose versus half-dose versus half-dose-half-fluence. *Graefes Arch Clin Exp Ophthalmol*. 2019;257(10):2155–2161.
14. Razavi S, Souied EH, Cavallero E, Weber M, Querques G. Assessment of choroidal topographic changes by swept source optical coherence tomography after photodynamic therapy for central serous chorioretinopathy. *Am J Ophthalmol*. 2014;157(4):852–860.
15. Maruyama K, Mei S, Sakaguchi H, et al. Diagnosis of choroidal disease with deep learning-based

image enhancement and volumetric quantification of optical coherence tomography. *Transl Vis Sci Technol*. 2022;11(1):22.
16. Nicholson B, Noble J, Forooghian F, Meyerle C. Central serous chorioretinopathy: update on pathophysiology and treatment. *Surv Ophthalmol*. 2013;58(2):103–126.
17. van Rijssen TJ, van Dijk EHC, Yzer S, et al. Central serous chorioretinopathy: towards an evidence-based treatment guideline. *Prog Retin Eye Res*. 2019;73:100770.
18. Mao Z, Miki A, Mei S, et al. Deep learning based noise reduction method for automatic 3D segmentation of the anterior of lamina cribrosa in optical coherence tomography volumetric scans. *Biomed Opt Express*. 2019;10(11):5832–5851.
19. Hojjatoleslami A, Avanaki MR. OCT skin image enhancement through attenuation compensation. *Appl Opt*. 2012;51(21):4927–4935.
20. Girard MJ, Strouthidis NG, Desjardins A, Mari JM, Ethier CR. In vivo optic nerve head biomechanics: performance testing of a three-dimensional tracking algorithm. *J R Soc Interface*. 2013;10(87):20130459.
21. Paris S, Hasinoff SW, Kautz J. Local Laplacian filters: edge-aware image processing with a Laplacian pyramid. *Commun ACM*. 2015;58(3):81–91.
22. Pizer SM, Amburn EP, Austin JD, et al. Adaptive histogram equalization and its variations. *Comput Vis Graph Image Process*. 1987;39(3):355–368.
23. Lefrère JJ, Sender A, Mercier B, et al. High rate of GB virus type C/HGV transmission from mother to infant: possible implications for the prevalence of infection in blood donors. *Transfusion*. 2000;40(5):602–607.
24. Sonoda S, Sakamoto T, Yamashita T, et al. Luminal and stromal areas of choroid determined by binarization method of optical coherence tomographic images. *Am J Ophthalmol*. 2015;159(6):1123–1131.e1.
25. Agrawal R, Chhablani J, Tan KA, Shah S, Sarvaiya C, Banker A. Choroidal vascularity index in central serous chorioretinopathy. *Retina*. 2016;36(9):1646–1651.
26. Duan L, Hong YJ, Yasuno Y. Automated segmentation and characterization of choroidal vessels in high-penetration optical coherence tomography. *Opt Express*. 2013;21(13):15787–15808.
27. Kajić V, Esmaeelpour M, Glittenberg C, et al. Automated three-dimensional choroidal vessel segmentation of 3D 1060 nm OCT retinal data. *Biomed Opt Express*. 2013;4(1):134–150.
28. Agrawal R, Salman M, Tan KA, et al. Choroidal vascularity index (CVI)—a novel optical coherence tomography parameter for monitoring patients with panuveitis? *PLoS One*. 2016;11(1):e0146344.
29. Zhou H, Dai Y, Shi Y, et al. Age-related changes in choroidal thickness and the volume of vessels and stroma using swept-source OCT and fully automated algorithms. *Ophthalmol Retina*. 2020;4(2):204–215.
30. Childs H, Brugger E, Whitlock B, et al. VisIt: an end-user tool for visualizing and analyzing very large data. In: Bethel EW, Childs H, Hansen C, eds. *High Performance Visualization: Enabling Extreme-Scale Scientific Insight*. Boca Raton, FL: CRC Press; 2012:358–372.
31. Ruiz-Medrano J, Flores-Moreno I, Peña-García P, Montero JA, Duker JS, Ruiz-Moreno JM. Macular choroidal thickness profile in a healthy population measured by swept-source optical coherence tomography. *Invest Ophthalmol Vis Sci*. 2014;55(6):3532–3542.
32. Manabe S, Shiragami C, Hirooka K, Izumibata S, Tsujikawa A, Shiraga F. Change of regional choroid thickness after reduced-fluence photodynamic therapy for chronic central serous chorioretinopathy. *Am J Ophthalmol*. 2015;159(4):644–651.
33. Burumcek E, Mudun A, Karacorlu S, MO Arslan. Laser photocoagulation for persistent central serous retinopathy: results of long-term follow-up. *Ophthalmology*. 1997;104(4):616–622.
34. Yannuzzi LA, Slakter JS, Kaufman SR, Gupta K. Laser treatment of diffuse retinal pigment epitheliopathy. *Eur J Ophthalmol*. 1992;2(3):103–114.
35. Sato-Akushichi M, Ono S, Klose G, Song Y. Choroidal volume evaluation after photodynamic therapy using new optical coherence tomography imaging algorithm. *Pharmaceuticals (Basel)*. 2021;14(11):1140.
36. Sonoda S, Sakamoto T, Kakiuchi N, et al. Semi-automated software to measure luminal and stromal areas of choroid in optical coherence tomographic images. *Jpn J Ophthalmol*. 2018;62(2):179–185.
37. Ogawa Y, Maruko I, Koizumi H, Iida T. Quantification of choroidal vasculature by high-quality structure en face swept-source optical coherence tomography images in eyes with central serous chorioretinopathy. *Retina*. 2020;40(3):529–536.
38. Yang J, Wang E, Yuan M, Chen Y. Three-dimensional choroidal vascularity index in acute central serous chorioretinopathy using swept-source optical coherence tomography. *Graefes Arch Clin Exp Ophthalmol*. 2020;258(2):241–247.

39. Izumi T, Koizumi H, Maruko I, et al. Structural analyses of choroid after half-dose verteporfin photodynamic therapy for central serous chorioretinopathy. *Br J Ophthalmol*. 2017;101(4):433–437.
40. Iovino C, Au A, Chhablani J, et al. Choroidal anatomic alterations after photodynamic therapy for chronic central serous chorioretinopathy: a multicenter study. *Am J Ophthalmol*. 2020;217:104–113.
41. Zhou H, Bacci T, Freund KB, Wang RK. Three-dimensional segmentation and depth-encoded visualization of choroidal vasculature using swept-source optical coherence tomography. *Exp Biol Med (Maywood)*. 2021;246(20):2238–2245.
42. Zhou H, Chu Z, Zhang Q, et al. Attenuation correction assisted automatic segmentation for assessing choroidal thickness and vasculature with swept-source OCT. *Biomed Opt Express*. 2018;9(12):6067–6080.
43. Breher K, Terry L, Bower T, Wahl S. Choroidal biomarkers: a repeatability and topographical comparison of choroidal thickness and choroidal vascularity index in healthy eyes. *Transl Vis Sci Technol*. 2020;9(11):8.
44. Agrawal R, Gupta P, Tan KA, Cheung CM, Wong TY, Cheng CY. Choroidal vascularity index as a measure of vascular status of the choroid: measurements in healthy eyes from a population-based study. *Sci Rep*. 2016;6:21090.